

4. Conference on nuclear cross sections and technology. Washington, US, 3-7 March 1975  
CEA-CONF--3057

THE TOTAL CROSS SECTION AND THE FISSION CROSS SECTION OF  $^{241}\text{Am}$   
IN THE RESONANCE REGION. RESONANCE PARAMETERS.

H. Derrien and B. Lucas

Département de Physique Nucléaire  
CEN Saclay, BP 2, 91190 Gif-sur-Yvette, France

The  $^{241}\text{Am}$  total and fission cross sections have been measured in the resonance region, using the 60 MeV Saclay linac as a pulsed neutron source. The resonance parameters obtained by a single level shape analysis of the transmission data are given for 189 levels up to 150 eV neutron energy. The mean level spacing, corrected for 18 % of missed resonances in the 0 to 50 eV energy range, is  $(0.55 \pm 0.05)$  eV. The s-wave neutron strength function value, in the 0 to 150 eV energy range, is equal to  $(0.94 \pm 0.09)10^{-4}$ . The average radiation width obtained from 43 resonances is  $(43.77 \pm 0.72)$  meV. Only preliminary results of the fission experiment are available now ; 38 fission widths are given up to 32 eV neutron energy, with the average value  $\langle \Gamma_f \rangle = 0.23$  meV ; the statistical distribution of these fission widths corresponds to a  $\chi^2$  law with 4 degrees of freedom. An area analysis of the Los Alamos fission data has also been done, from which we obtain 36  $\Gamma_f$  values in the 20 eV to 50 eV energy range ; the corresponding average value is :  $\langle \Gamma_f \rangle = 0.52$  meV ; the statistical distribution obeys to a  $\chi^2$  law with 15 degrees of freedom, in disagreement with the Saclay results.

The Total Cross Section Measurement and Analysis

Experimental Conditions

The total cross section has been obtained up to 1 keV neutron energy from the transmission measurements of three sample thicknesses of americium oxide :  $0.18 \text{ g/cm}^2$ ;  $0.63 \text{ g/cm}^2$  and  $(0.63 + 1.24) = 1.87 \text{ g/cm}^2$ . Three series of measurement were performed : the first at a 17 m flight path and the others at a 53 m flight path. The main characteristics of each series are given in the table 1. The best nominal resolution achieved was  $0.8 \text{ ns/m}$ .

Table 1

Energy range (eV)	Channel width (ns)	Electron burst width (ns)	Flight path length (m)	Sample thickness ( $\text{g/cm}^2$ )
0.8-3.5	640			
3.5-8.8	320			
8.8-20	160	100	17.9	0.18, 0.63 and 1.87
20-27	80			
27-90	80	100	53.4	1.87
90-150				
150-1000	50	10	53.4	1.87

Methed of Analysis

A shape analysis of the experimental data has been done up to 150 eV neutron energy by a least square fit (the code used is described in reference 2), which gives the energies, the neutron widths and the total widths of the resonances. In this shape analysis, the theoretical function is a sum of single level Breit-Wigner formulae broadened by a gaussian Doppler function and by a gaussian resolution. Such a formulation of the cross section gives a good representation of the resonance shape since the interferences in the fission channels are negligible (very small value of the fission widths). The Doppler width is taken equal to  $0.0209 \sqrt{E}$  ( $E$  energy of the incident neutron) with an accuracy better than 2 %. The parameters obtained by this analysis are given in table 2. In this table  $\Delta(2g\Gamma_n)_1$  corresponds to the statistical error and  $\Delta(2g\Gamma_n)_2$  to the systematic error due to the background evaluation ;  $\Delta(\Gamma_\gamma)$  is a statistical error.

Level Spacings

A number of 189 resonances is identified in the 0 to 150 eV energy range (including the resonances at 0.308 eV and 0.576 eV)<sup>3</sup>.

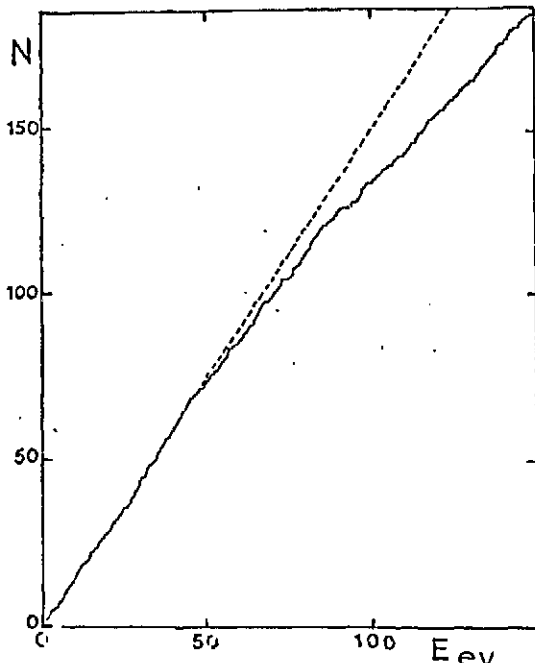


Fig. 1

Figure 1 shows the cumulative sum of the number of levels  $N$  versus the neutron energy  $E$ , in this energy range ; beyond 50 eV the variation of  $N$  is not linear ; there is a loss of resonances due to the increasing Doppler and resolution widths. So, a statistical study of the resonance parameters has to be limited to the 78 levels of the 0 to 50 eV energy range ; in this interval the observed mean spacing is equal to 0.65 eV.

Table 2

$E$ (eV)	$\Delta E_{\text{h}}$ (eV)	$\Delta(E_{\text{h}})_1$ (eV)	$\Delta(E_{\text{h}})_2$ (eV)	$T_x$ (eV)	$\Delta T_x$ (eV)	$E$ (eV)	$\Delta E_{\text{h}}$ (eV)	$\Delta(E_{\text{h}})_1$ (eV)	$\Delta(E_{\text{h}})_2$ (eV)	$T_y$ (eV)	$\Delta T_y$ (eV)
0.308	0.110	0.004				62.019	4.002	0.644	0.074	47.1	4.6
0.374	0.175	0.007				64.530	1.054	0.652	0.075	50.3	9.2
1.276	0.137	0.009	0.026	46.5	0.8	65.154	5.197	0.648	0.102	49.7	3.7
1.372	0.111	0.011	0.026	46.4	0.3	65.735	1.340	0.614	0.010	18.4	14.0
2.372	0.073	0.011	0.004	47.6	0.3	66.114	1.014	0.652	0.010	75.2	19.6
2.598	0.147	0.001	0.010	46.0	0.3	66.773	2.104	0.644	0.075	71.9	8.1
3.673	0.210	0.001	0.005	46.5	0.3	67.525	0.631	0.019	0.003		
4.918	0.175	0.001	0.004	47.8	0.4	69.565	1.114	0.651	0.013		
5.615	0.160	0.001	0.018	46.2	0.1	70.924	2.061	0.653	0.040		
5.800	0.002					71.593	0.583	0.655	0.006		
6.117	0.126	0.001	0.002	43.8	0.7	71.613	1.109	0.679	0.111		
6.745	0.124	0.001				71.461	1.017	0.625	0.010		
7.659	0.037	0.001				72.276	0.725	0.021	0.001		
8.173	0.104	0.001	0.001	47.7	1.7	74.569	0.681	0.020	0.004		
9.113	0.319	0.002	0.009	44.2	0.6	75.715	0.374	0.036	0.003		
9.851	0.400	0.002	0.009	43.4	0.6	76.043	0.515	0.027	0.003		
10.114	0.220	0.001				76.779	0.162				
10.403	0.224	0.002	0.005	42.4	0.8	78.191	1.044	0.049	0.015	10.3	17.4
10.997	0.413	0.002	0.006	46.5	0.8	78.551	1.178	0.105	0.011	60.8	24.0
11.583	0.016	0.001				79.555	0.730	0.023	0.005		
12.137	0.007	0.001				80.050	0.544	0.024	0.004		
12.879	0.131	0.001	0.001			80.393	0.584	0.029	0.004		
13.874	0.012	0.001				81.077	0.106	0.039			
14.360	0.071	0.002	0.001			81.458	1.042	0.051	0.001	104.4	35.0
14.682	2.482	0.011	0.075	40.3	0.5	82.049	1.454	0.054	0.015	28.7	14.0
15.689	0.244	0.003	0.003	39.3	2.9	82.900	0.439	0.024	0.003		
16.388	1.277	0.005	0.034	41.5	0.9	83.370	0.431	0.024	0.004		
16.849	0.644	0.012		41.2	1.5	84.006	1.456	0.027	0.015	38.1	8.7
17.729	0.391	0.004	0.006	37.3	2.4	84.685	2.141	0.044	0.022		
18.167	0.017					86.610	0.225	0.025	0.001		
19.445	0.213	0.003	0.002			87.481	0.125	0.029			
20.333	0.034					87.984	3.919	1.051	0.055	70.7	6.3
20.680	0.080	0.001				89.297	0.332	0.061	0.002		
21.760	0.091	0.003				89.602	2.364	0.023	0.024	86.7	16.1
22.768	0.069	0.003				93.412	6.295	0.055	0.115	53.7	4.0
23.079	0.417	0.012	0.005	42.2	4.0	94.610	0.754	0.032	0.006		
23.337	0.445	0.012	0.006	42.5	5.8	95.295	0.340	0.035	0.003		
24.192	1.302	0.017	0.028	36.2	1.5	95.586	2.463	0.021	0.034		
25.004	0.010	0.001	0.001			96.100	2.904	0.048	0.017		
25.634	1.258	0.001	0.025	37.6	1.7	96.440	2.834	0.052	0.035		
26.498	0.487	0.014	0.006	22.0	4.1	97.423	0.277	0.030	0.001		
26.669	0.217	0.010	0.014			99.356	0.245	0.030	0.001		
27.575	0.165	0.021	0.002			100.156	1.075	0.033	0.009		
27.724	0.509	0.029	0.006	70.6	8.8	101.599	2.825	0.058	0.028	51.1	10.0
28.355	0.510	0.034	0.008	44.7	3.7	102.555	0.248	0.035	0.001		
28.903	0.461	0.009	0.004	48.6	4.7	103.203	6.480	0.063	0.120	40.2	4.5
29.594	0.771	0.009	0.009	44.6	3.2	104.740	2.196	0.059	0.022	40.2	12.8
29.954	0.050					104.148	5.824	0.185	0.194		
30.872	0.150	0.010	0.002			106.336	3.352	0.180	0.054		
31.020	0.334	0.030	0.004			107.615	1.925	0.038	0.019		
31.251	0.794	0.014	0.015	42.6	4.2	109.126	3.256	0.144	0.042		
32.030	0.300	0.010	0.003	47.4	8.6	110.093	3.337	0.144	0.043		
33.510	0.060					111.170	0.374	0.059	0.003		
34.028	0.424	0.012	0.008	45.4	4.9	111.427	5.200	0.132	0.068	94.3	10.4
34.460	0.125	0.007				112.752	0.414	0.042	0.003		
34.928	0.612	0.012	0.006	42.4	5.4	113.280	0.300				
35.445	0.427	0.012	0.004	50.6	8.1	113.907	1.741	0.070	0.014	77.6	23.0
36.422	0.157	0.007	0.001			114.084	1.400	0.061	0.014	79.3	23.8
36.443	0.100					115.777	0.731	0.049	0.004		
36.977	2.495	0.017	0.075	52.0	1.5	116.398	2.623	0.051	0.023	42.0	15.4
38.368	2.260	0.015	0.044	47.0	2.0	117.656	0.030				
38.830	0.055					118.522	0.804	0.046	0.005		
39.617	1.275	0.020	0.020	40.2	4.2	119.873	2.237	0.131	0.022		
40.067	0.541	0.040	0.005	77.9	20.1	120.123	1.930	0.131	0.026		
40.395	0.944	0.034	0.012	66.0	8.6	121.692	3.216	0.134	0.033	36.9	19.0
41.248	0.044					122.552	3.953	0.272	0.040	64.2	27.6
41.741	0.355	0.009	0.003			123.243	3.534	0.165	0.035	56.3	20.5
42.130	0.150	0.009	0.001			124.944	1.640	0.054	0.011		
43.254	0.805	0.031	0.010	18.0	8.9	125.919	1.015	0.055	0.007		
43.574	0.542	0.035	0.004	36.2	13.6	126.461	2.035	0.057	0.017		
44.416	0.119	0.009				127.415	0.250				
44.421	0.074	0.009				127.944	1.040	0.056	0.013		
46.073	0.645	0.018	0.007	43.8	8.6	129.477	0.225				
46.566	0.371	0.010	0.003	22.8	14.0	130.770	1.158	0.072	0.009		
47.535	1.053	0.017	0.012	41.6	5.2	131.319	3.121	0.172	0.032	56.0	23.2
48.765	0.711	0.018	0.007	40.0	8.0	132.180	0.975	0.062	0.006		
49.332	0.220	0.011	0.002			132.754	1.180	0.059	0.008		
50.278	2.442	0.022	0.042	51.8	3.0	133.657	1.784	0.100	0.014	52.1	30.5
50.847	0.303	0.020	0.003	35.8	16.4	134.967	0.615	0.317	0.104		
51.934	1.308	0.021	0.017	50.2	4.9	135.469	4.131	0.348	0.042		
53.014	0.165	0.012	0.001			136.435	5.757	0.145	0.068	45.7	14.1
53.443	0.164	0.012	0.001			137.103	1.292	0.077	0.009		
54.407	0.073					137.613	1.628	0.064	0.012		
54.490	1.443	0.025	0.002	108.5	6.9	138.774	3.684	0.108	0.040	40.6	15.4
55.593	0.713	0.014	0.002			139.963	1.253	0.071	0.008		
55.945	1.432	0.034	0.018			140.498	2.434	0.073	0.021		
56.158	0.949	0.034	0.010			141.310	4.229	0.109	0.055		
57.372	4.166	0.029	0.002	81.0	2.7	141.520	3.256	0.106	0.039		
59.066	0.589	0.028									

Figure 2 shows the corresponding distribution of the level spacings ; the dashed line represents the Wigner distribution (two populations with spin and parity  $J^\pi = 2^+$  and  $J^\pi = 3^-$ ) normalized to the area of the experimental histogram. There is no agreement between the theoretical and the experimental distributions, which is an usual result for a nucleus with such a small level spacing ; the same kind of discrepancy is observed for  $^{233}\text{U}$ ,  $^{235}\text{U}$ ,  $^{241}\text{Pu}$ ,  $^{237}\text{Np}$  ... and is mainly due to the resonance overlap hiding the small resonances.

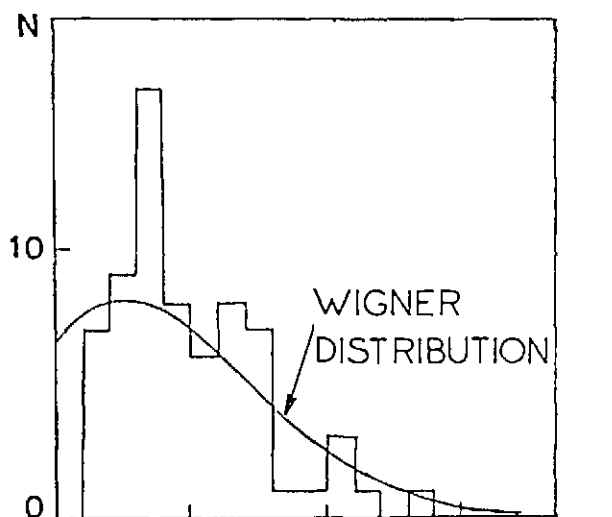


Fig. 2

#### Neutron Widths and S-Wave Strength Function

The distribution of the reduced neutron widths for resonances between 0 and 50 eV agrees relatively well with the Porter-Thomas law, if one assumes that about 15 % of levels are missed, corresponding to  $\Gamma_n^0$  values smaller than 0.1 times the mean value.

The strength function  $S_0$  is evaluated by the relation :

$$S_0 = \frac{\int_{E_1}^{E_2} \frac{2g\Gamma_n^0(E)}{2(E_2 - E)} dE}{\int_{E_1}^{E_2} dE};$$

the value obtained is not affected by the missed levels since in the shape analysis we take into account the total area of non resolved resonances. We obtain :  $S_0 = (0.75 \pm 0.12)10^{-4}$  in the 0-50 eV energy range and  $S_0 = (0.94 \pm 0.09)10^{-4}$  in the 0-150 eV energy range.

G.G. SLAUGHTER et al.<sup>4</sup> give a value of  $(1.1 \pm 0.2)10^{-4}$  from an area analysis of the total cross cross section as measured by BLOCK et al.<sup>5</sup>, up to about 45 eV. This value is significantly higher than ours ; the discrepancy is mainly due to three resonances or group of resonances (6.74 eV ; 9.17 eV and = 43 eV) for which SLAUGHTER proposed  $\Gamma_n^0$  values about ten times greater than ours.

#### Capture Widths

The capture widths  $\Gamma_y$  have been obtained for a large number of resonances by the relation :

$\Gamma_y = \Gamma - 2g\Gamma_n^0$ , assuming that  $\Gamma_n^0$  and  $\Gamma_f$  are small enough. Up to 50 eV neutron energy the  $\Gamma_y$  values are obtained with a relatively good accuracy ; beyond, the values are much more scattered, due to the facts that : i) the shape analysis cannot give accurate values of  $\Gamma$  when the Doppler and the resolution function widths are too large compared to  $\Gamma$  ; ii) the probability of observing unresolved resonances increases with energy, likewise the probability of observing abnormal large  $\Gamma$  values. The weighted average value in the 0 to 50 eV energy interval is :  $\langle\Gamma_y\rangle = (43.77 \pm 0.72)$  meV, which is mainly due to the very accurate values in the 0 to 10 eV energy interval ; a correction of 0.20 meV has been applied to the average value to take into account the fission widths.

#### Attempt to Determine the Number of Missed Levels

The examination of the level spacing and neutron width distributions shows that 15 % to 20 % of levels are missed in the experimental cross section. A more precise evaluation of the number of missed levels has been done by a Monte-Carlo method. Table 3 shows the results obtained for 9 calculated cross sections in the 0 to 50 eV energy range, which are supposed to have the same statistical properties as  $^{241}\text{Am}$ .

Table 3

	N	D (eV)	$N_{\text{obs}}$	$D_{\text{obs}}$ (eV)	$\frac{N-N_{\text{obs}}}{N}$
1	81	0.61	67	0.74	17 %
2	98	0.51	79	0.63	20 %
3	84	0.60	70	0.71	17 %
4*	88	0.57	74	0.67	16 %
5	89	0.56	74	0.67	16 %
6	102	0.49	80	0.62	22 %
7*	89	0.56	73	0.70	18 %
8*	95	0.53	75	0.67	21 %
9	91	0.54	72	0.68	21 %

N = number of levels for the calculated cross section.

$N_{\text{obs}}$  = number of observed levels.

The cases n° 4, 7 and 8 have been particularly studied ; from a total number of 272 levels, 222 are observed, which means 18 % of missed levels ; the 50 non observed resonances correspond to 11 doublets (4 %) with large  $\Gamma_n^0$  values and 39 (14 %) with  $\Gamma_n^0$  values less than 0.1  $\langle\Gamma_n^0\rangle$  ; 13 % of the missed level spacing are smaller than 0.4  $\langle D \rangle$ .

The conclusion is : the observed mean spacing has to be corrected for  $(18 \pm 4)$  % missed resonances ; then the right value of the average spacing would be :  $\langle D \rangle = (0.55 \pm 0.05)$  eV.

#### Fission Cross Section Measurements. Preliminary Results

##### Experimental Conditions

Due to the strong  $\alpha$  activity of  $^{241}\text{Am}$ , a fission fragment detector is not suitable for such measurement. We have built a new detector based on the fission neutron detection, using NE 213 as liquid scintillator. The  $\gamma$ -ray pulses are eliminated by a pulse shape discrimination method.<sup>6</sup> The rejecting rate for  $\gamma$ -ray pulses was  $10^5$ . An anti pile up system has been used and only isolated pulses in 1  $\mu\text{s}$  interval are taken into account. The detector has a cylindrical geometry and

contains 45 liters of liquid in 4 optically independent parts, each part being viewed by a XP 1040 photomultiplier. Internal shielding of lead and natural boron was used to protect against a large fraction of the  $\gamma$ -rays coming from the sample, and against neutrons thermalized in the liquid and backscattered. Due to the anti pile up system, the efficiency of the detector depends on the activity of the sample ; for  $^{241}\text{Am}$ , it is about 8 %. The energy threshold for the detection of fission neutrons is 800 keV, and the time resolution 5 ns.

The results given in this section concern only a preliminary experiment, for which the experimental conditions are those shown in Table 4.

Table 4

Energy range (eV)	TOF analyser width (ns)	Linac electron pulse width : 100 ns Frequency pulse : 500 Hz Sample thickness : 0.17 g/cm <sup>2</sup> Counting-rate : 10 fissions/h in the 5.4 eV resonance peak Experiment duration : 200 h
0.8-3.8	800	
3.8-9.7	400	
9.7-23.6	200	
26.6-86.7	100	
86.7-152	50	

#### Results

The normalization has been done in relation to the BOWMAN results<sup>7</sup> (spark chamber measurement) which were normalized to the value of 3.13b at 0.025 eV neutron energy ; the resonance areas were compared for 11 levels up to 15 eV ; a good agreement can be obtained for 7 resonances, but not for the resonances at 3.97, 4.97, 6.12 and 9.11 eV for which the areas obtained from the parameters published by BOWMAN are about ten times smaller than ours. Nevertheless, there is no apparent discrepancy in the fission cross sections in the vicinity of these resonances. The origin of the disagreement has to be find in some mistake in the resonance analysis.

Table 5 - Fission widths from Saclay data.

E	$\Gamma_f$	E	$\Gamma_f$	E	$\Gamma_f$
1.78	0.37	10.12	0.14	24.19	0.14
1.93	0.09	10.40	0.06	25.63	0.29
2.37	0.14	10.94	0.13	26.50	0.05
2.60	0.17	12.89	0.04	26.67	0.19
3.97	0.16	14.68	0.27	28.36	0.16
4.97	0.44	15.49	0.10	28.90	0.16
5.42	0.63	16.39	0.11	29.50	0.10
6.12	0.42	16.85	0.32	31.25	0.22
6.74	0.22	17.73	0.30	32.03	0.28
7.64	0.10	19.44	0.03	36.98	0.51
8.17	0.12	21.74	0.27	38.37	0.30
9.11	0.18	23.04	0.27	39.62	0.23
9.85	0.95	23.34	0.17		

Table 5 shows the  $\Gamma_f$  values obtained for 38 resonances up to 32 eV ; these values were calculated by the relation :  $\Gamma_f = \Gamma_x (A_f / A_t)$  ;  $A_f$  and  $A_t$  are the fission and the total areas ;  $\Gamma$  and  $A_t$  correspond to the parameters of Table 2. The average fission width is :  $\langle \Gamma_f \rangle = 0.23$  meV. The integral distribution shown in figure 3 is well represented by a  $\chi^2$  law with 4 degrees of freedom. That mean that there is a quite large

number of channels contributing to the  $^{241}\text{Am}$  sub-threshold fission, which is not impossible, since the  $^{242}\text{Am}$  compound nucleus is an odd-odd one.

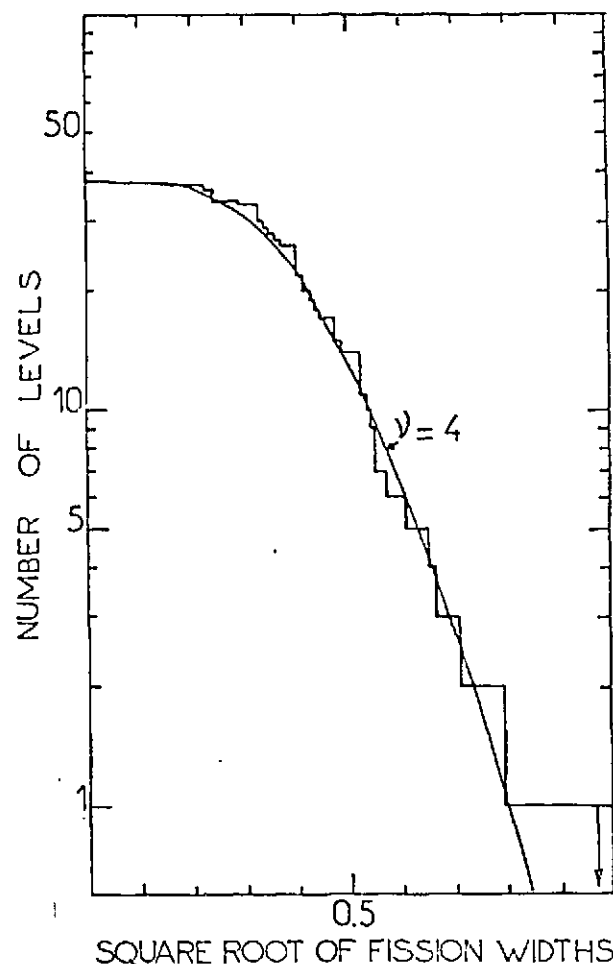


Fig. 3

#### The Fission Widths Deduced of the Los Alamos Fission Cross Section<sup>1</sup> in the 20 eV to 50 eV Energy Range

No fission widths have been published up to now from the Los Alamos fission data. We have analysed these data (provided by the CCDN at Saclay) between 20 eV and 50 eV . Table 6 shows the fission widths we

Table 6 - Fission widths from Los Alamos data.

E	$\Gamma_f$	E	$\Gamma_f$	E	$\Gamma_f$
22.75	0.58	30.62	1.20	40.07	0.79
23.09	0.77	31.02	0.51	40.41	0.34
23.34	0.31	31.25	0.57	43.29	0.35
24.19	0.48	32.03	0.56	43.57	0.49
25.63	0.82	34.03	0.22	46.07	0.27
26.50	0.47	34.46	0.74	46.57	0.28
26.67	0.49	34.93	0.41	47.54	0.25
27.57	2.54	35.49	0.36	48.76	0.49
27.73	0.44	36.25	0.57	49.33	0.54
28.36	0.55	36.99	0.46	50.28	0.37
28.90	0.36	38.37	0.53	50.65	0.47
29.50	0.45	39.62	0.46	51.98	0.38

obtained for 36 resonances. The corresponding average value is :  $\langle \Gamma_f \rangle = 0.52$  meV, which is larger than the Saclay average value by a factor 2.3. The distribution of these fission widths is shown in figure 4 ; it corresponds to a  $\chi^2$  law with 15 degrees of freedom, not in agreement with the fission channel theory.

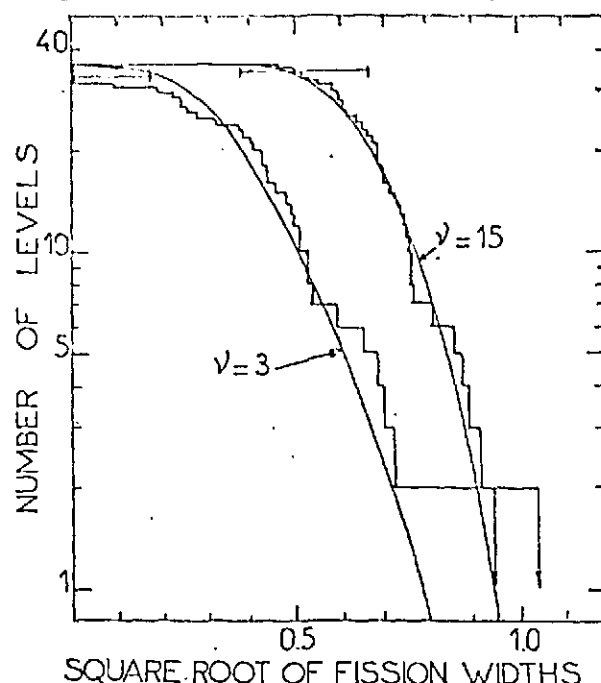


Fig. 4

The discrepancy between the average fission widths could be explained by a defect of normalization. As a matter of fact, the fission integral in the 22.5 eV to 28.7 eV energy range is equal to 2.32b-eV ; 2.80b-eV or 6.48b-eV when evaluated from Saclay, BOWMAN or Los Alamos data, which means that no severe discrepancy would appear in the average fission width if the Los Alamos results were renormalized to the Saclay or BOWMAN data. But such a renormalization will not change the shape of the Los Alamos fission width distribution ; particularly, the number of degrees of freedom will remain the same. Another explanation is a possible contamination by capture events in the Los Alamos experiment ; but to explain the observed discrepancy the contamination would be relatively important ; we have shown on the figure 4 how a correction of 0.30 meV on each fission width would modify the fission width distribution, which then would correspond to about 3 degrees of freedom. In this case, the Los Alamos measured cross section would be a mixing of 40 % fission and 60 % capture (in the average) ; however this capture contribution represents only 0.7 % of the total capture.

#### References

- 1 P.A. SEEGER et al., Nucl. Phys., 1967, A96, 605.
- 2 P. RIBON et al., Conf. AIEA sur les Données Nucléaires pour les Réacteurs, Paris 1966, CN 23/71.
- 3 BNL-325, 2th edition, supplément n° 2, vol. III.
- 4 G.G. SLAUGHTER et al., ORNL-3085, 1961.
- 5 R.C. BLOCK et al., ORNL-2718, 1959.
- 6 R.B. OWEN, AERE EL/R-2712, 1958.
- 7 C.D. BOWMAN et al., Phys. Rev., 1965, 137, B326.